



Enhancement of Buckling Resistance of Aluminized Long Columns of Stainless Steel AISI 303

Ahmed Naïf Al-Khazraji*

Samir Ali Al-Rabii**

Hameed Shamkhi Al-Khazalli***

*,** Department of Mechanical Engineering / University of Technology

**Department of Machines and Equipment / Institute of Technology / Middle Technical University / Baghdad

*Email: dr_ahmed53@yahoo.com

*Email: alrabiee202@yahoo.com

***Email: hameedshamkhi@yahoo.com

(Received 11 June 2015; accepted 4 August 2015)

Abstract

This paper has investigated experimentally the dynamic buckling behavior of AISI 303 stainless steel Aluminized and as received long columns. These columns, hot-dip aluminized and as received, are tested under dynamic buckling, 22 specimens, without aluminizing (type 1), and 50 specimens, with hot-dip aluminizing at different aluminizing conditions of dipping temperature and dipping time (type 2), are tested under dynamic compression loading and under dynamic combined loading (compression and bending) by using a rotating buckling test machine. The experimental results are compared with Perry Robertson interaction formula that used for long columns. Greenhill formula is used to get a mathematical model that describes the buckling behavior of the specimens of type (1) under dynamic compression loading. The experimental results obtained show an advantageous influence of hot-dip aluminizing treatment on dynamic buckling behavior of AISI 303 stainless steel long columns. The improvement based on the average value of critical buckling stress, are as follow: (64.8 %) for long columns type (2), compared with columns type (1), under dynamic compression loading, and (56.6 %) for long columns type (2), compared with columns type (1), under dynamic combined loading, and (33.3 %) for long columns type (2) compared with Perry Robertson critical buckling stress.

Keywords: Dynamic buckling, hot-dip Aluminizing, long columns, AISI 303 stainless steel.

1. Introduction

Structural members subjected to axial compressive loads may fail in a manner that depends upon their geometrical properties rather than material properties [1]. It common experience, for example, that a long slender structural member will suddenly bow with large lateral displacements when subjected to an axial compression load [1, 2]. Long slender members subjected to an axial compressive force are called columns, and the lateral deflection that occurs is called buckling [3]. The buckling behavior of steel columns consider one of the important

phenomenon that had been studying and analysis from a long time. For combined axial and bending loads, European standard (Eurocode 3 ENV 1939-1-4), American standard (SEI/ASCE 8-02), and Australian/ New Zealand standard (AS/NZE 4673 are suggested to use the guidance developed for carbon steel to determine the resistance of stainless steel members [4]. A series of experimentally tests are carried on cold formed austenitic stainless steel square, rectangular, and circular hollow section members to examine the buckling behavior of columns and beams under effect of gradually increased single and combined loads (compression, bending, and compression-bending) with two types of ends conditions pin-

ends and fixed-ends [5]. The buckling of solid and hollow CK35 and CK45 alloy steel columns under combined dynamic loading has been studied experimentally and the obtained results showed that the failure resistance of the columns depends on the type of cross-section and initial deflection of column [6]. The nitride case hardening (liquid nitriding) surface treatment is used to enhance the buckling resistance of square columns with different length, material (CK45, CK67, CK101), and constant cross section (10 ×10) mm subjected to the effect of single and combined dynamic loads. The results of the study showed experimentally that the resistance and the number of cycles to failure were increased by using this method [7]. The surface treatment by shot peening is used to enhance the buckling resistance of a series of (CK35) steel column with solid circular cross-section under single and combined dynamic loads by increasing the yield and ultimate strength of columns material [8]. Because of the many practical applications of stainless steel columns in constructions of the buildings, ships, bridges, airplanes, spaceships, etc., there were many of studies and researches to improve the buckling resistance of columns by using of number of methods, for example:

- Improvement of the mechanical properties of the columns material by using new special metal alloys, or by using of composite materials.
- Improvement of columns section design by using of the modern design methods that increases of the columns resistance to the buckling.
- Using of the surface treatments methods such as: shot-peening and heat treatment.

Surface coating is an efficient and economical way to obtain the desirable material properties by altering physical, chemical, or electrical characteristics of a material. Surface modification by coatings has become an essential step to improve the surface properties such as, resistance to wear, corrosion and oxidation [9, 10]. The influence of surface coating treatment on the surface properties and some of the mechanical properties was investigated by many researchers. A new pack cementation process technique was used to enhance the hot corrosion and oxidation resistance of stainless steel AISI 316L by using two different kinds of coating, the first one was Si-modified aluminide coating and the second was the Ce-doped silicon modified aluminide coating [11]. Hot dip aluminizes samples with (1-6 wt %) silicon concentration of aluminizing melt and

samples aluminized in pure aluminum were tested by using a 3-point bend device in order to compare the relative ductility and formability of the aluminized steel and to determine the influence of silicon concentration and coating thickness on these properties [12]. There are many fields of practical applications that needs to use of steel columns meet between the strength and resistance of the external environment conditions (corrosion, wear, and high temperature oxidation). From this point of design, the designer used numbers of procedures to maintain the above requirements. The surface coating by using aluminum (aluminizing process) was one of the popular methods to develop protection layer for substrate material from environment conditions. This paper examine the effect of hot-dip aluminizing process (HDA) on dynamic buckling of long columns subjected to compression and compression-bending loads, of stainless steel (AISI 303) material by series of circular cross-section columns, of different slenderness ratio, with and without HDA surface treatment at different dipping temperatures (T_{HD}) and dipping times (t_{HD}).

2. Theory

2.1. Perry Robertson Interaction Formula

It is important to evaluate the compressive buckling strength of real columns, σ_{cr} , in the presence of initial mechanical and geometrical imperfections, a Perry Robertson interaction formula [4, 13, 14, and 15] is adopted as follow:

$$\sigma_{cr} = \chi \sigma_y \quad \dots (1)$$

$$\text{and} \quad P_{cr} = A \times \sigma_{cr} \quad \dots (2)$$

where:

$$\chi = \frac{1}{\varphi + [\varphi^2 - (\bar{\lambda})^2]^{0.5}} \leq 1 \quad \dots (3)$$

in which:

$$\varphi = 0.5 (1 + \alpha(\bar{\lambda} - \bar{\lambda}_o) + (\bar{\lambda})^2) \quad \dots (4)$$

$$\bar{\lambda} = \frac{\lambda_e}{\pi} \cdot \sqrt{\frac{\sigma_y}{E}} \quad \dots (5)$$

Where the value of the imperfection factor (α) and the limiting non-dimensional slenderness ratio are defined in Table (1). The value of the effective slenderness ratio (λ_e) is calculated by using the relation [3]:

$$\lambda_e = \frac{KL}{r} = \frac{L_e}{r} \quad \dots (6)$$

The value of slenderness ratio above which column's type is long is obtained using the following relation [16]:

$$\lambda_c = \lambda_e = \pi \cdot \sqrt{\frac{E}{\sigma_{pl}}} \quad \dots (7)$$

and by substituted the value of E, σ_{pl} from Table (2), and the value of K=0.7 (for fixed-pinned ends) in Eq. (7), we find that the value of critical slenderness ratio is $\lambda_c = 86.5$.

Table 1,
Values of imperfection factor and limiting slenderness ratio for flexural, torsional and torsional- flexural buckling [14].

Buckling mode	Type of member	α	$\bar{\lambda}_0$
Flexural	Cold formed open sections	0.49	0.40
	Hollow sections (welded and seamless)	0.49	0.20
	Welded open sections (major axis)	0.78	0.20
	Welded open sections (minor axis)		
Torsional and torsional-flexural	All members	0.34	0.20

2.2. Spatial Buckling Under Torque and Axial Force

Spatial buckling of twisted and compressed shafts is important for the design of rotors of turbines, generators, and other rotating machinery. Spatial buckling may also be important for frames. Recently, design of latticed struts that can be collapsed for transport by means of torsion became of interest for construction of an orbiting space station [17].

Consider a geometrically perfect beam or shaft supported on two spherical hinges, loaded by axial force P and torque M_t , which is assumed to keep its direction during buckling; see Fig. (3-10), where the axial vector of torque is represented by a double arrow. According to Greenhill (1883), the relation between the buckling load P and torque M_t is given by [17].

$$\frac{P}{P_{cr}^0} + \left(\frac{M_t}{M_{cr}^0}\right)^2 = 1 \quad \dots (8)$$

where

$$P_{cr}^0 = \frac{\pi^2 EI}{L^2} \quad M_{cr}^0 = k \frac{\pi EI}{L} \quad \dots (9)$$

P_{cr}^0 is the critical load for buckling without torque (Euler formula), and M_{cr}^0 is the critical torque for buckling without axial force. Equation (8) is plotted in Fig. (1). By using effective length (L_e) instead of (L),

Eq. (8) can be used to determine the theoretical buckling load (P) for other form of ends support.

From Eqs. (8) and (9), one can be write

$$P = \left(1 - \left(\frac{M_t}{M_{cr}^0}\right)^2\right) * P_{cr}^0 \quad \dots (10)$$

and

$$k = \frac{M_t * L_e}{\pi EI * \left(1 - \frac{P}{P_{cr}^0}\right)^{1/2}} \quad \dots (11)$$

In this work, k consider as a function of buckling parameters in order to fit the experimental results with a mathematical model.

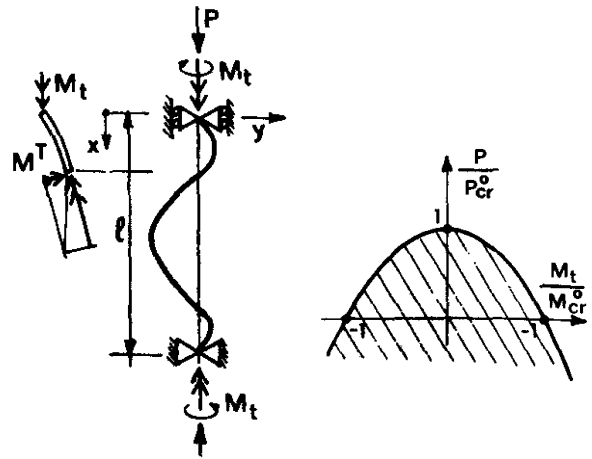


Fig. 1. Beam or shaft subjected to axial force and constant-direction torque [17].

3. Experimental Work

3.1. Material Used and Buckling Test Machine

AISI 303 stainless steel as long columns of circular cross-section, $\varnothing=8$ mm, of different slenderness ratio (λ), with and without hot-dip aluminizing were tested by using rotating column buckling test machine capable to apply compression and compression-bending dynamic loads, with column ends support of fixed- pinned and rotating speed of 17 and 34 r.p.m. in this research it was used low speed (17 r.p.m) in all dynamic buckling experiments. The photograph of the rotating buckling test machine is shown in Fig. (2). More details of buckling test machine, used in this research, were found in Ref. [6]. The detail of the chemical composition of stainless steel; tested and standardized in State Company for Inspection and Engineering Rehabilitation (SIER)/ Baghdad by a certificate No. 1043/2013 at room temperature (25 °C) and relative humidity (60%), is shown in Table (2). Also, the significant

mechanical properties, tested in Central Organization for Standardization and Quality Control (C.O.S.Q.C.) / Baghdad, are given in Table (3). While the experiments of hot dip aluminizing AISI 303 stainless steel rods are carried out , by using a self-construction system of hot- dip aluminizing, Fig. (3), in State Company for Electrical Industries/Baghdad/ Unit of casting. A high purity aluminum (99 %) was used for dipping bath, and the process variables were dipping temperature and dipping time.

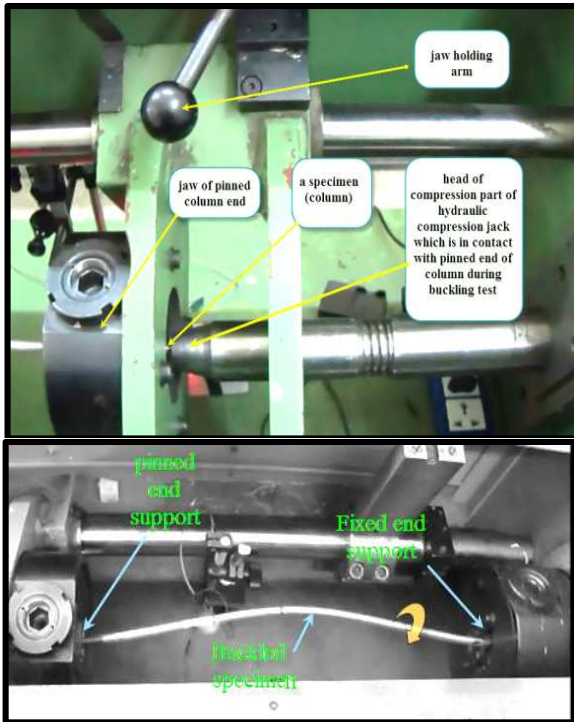


Fig. 2. The photograph of the rotating buckling test machine used in the present research.

Table 2, Chemical compositions (wt. %) of AISI 303 stainless steel.

Alloy	C	Si	Mn	P	Cr	Ni
Used material ^a	0.114	0.5	1.14	0.03	18.20	8.19
Standard (ASM) [18]	Up to 0.15	Up to 1.0	Up to 2.0	Up to 0.2	17-19	8-10

a: Source: State Company for Inspection and Engineering Rehabilitation (SIER)/Baghdad.

Table 3, Experimental mechanical properties of AISI 303 stainless steel used in present work (Average of three specimens)

AISI 303 st. st.	σ_{ult} (MPa)	σ_y^* (MPa)	E (GPa)	Elong.** (%)	σ_{pl} (MPa)
	880	673	204.2	41.4	269.2

* Proof stress at 0.2% of stain.

** In gauge length $L_o = 25\text{ mm}$.

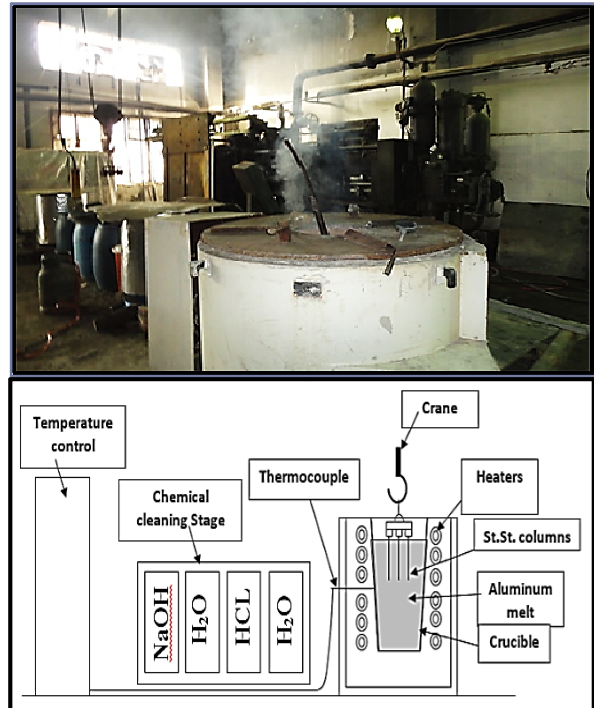


Fig. 3. Schematic diagram and photograph of the HDA system.

3.2. Specimens Types

There are two types of buckling specimens used in this work, these two types are:

Type (1) as received specimens (non-aluminized): columns with circular cross-section $D = 8\text{ mm}$, $I = 201.1\text{ mm}^4$, $r = 2\text{ mm}$, and different length. Table (4) gives the geometrical dimensions and buckling parameters of these specimens.

Type (2) aluminized specimens: hot-dip aluminized columns with circular cross-section. These specimens have a constant length $L=440\text{ mm}$, but at different hot-dip conditions from dipping temperature (700, 740, 780, 820, and 860 °C) and different dipping time (1, 2, 3, 4, and 5 minutes). Table (5) gives the parameters of hot-dip and buckling of these specimens.

3.3. Failure Criterion of Buckling

When the maximum deflection of the column reaches the critical value of deflection (δ_{cr}) of the column length, then the load measured (by pressure gauge) is the critical buckling load of the column. In the present work, the value of the critical deflection of the column is taken as

($\delta_{cr}(mm) = (L * 1\%) + \delta_o$) [18, 7, and 8]. Because of the rotating effect on the reading of the column deflection using a dial gauge, a laser cell circuit tool has been fabricated, with whistle sound, fixed on electronic vernier (with reading accuracy of 0.01 mm), Fig. (4), to make the reading of critical deflection (δ_{cr}) more strictness.

Table 4,
Geometrical dimensions and buckling parameters of specimens type (1).

No.	Symbol	L (mm)	L_e * (mm)	δ_o (mm)	δ_{cr} ** (mm)	λ_e ($\frac{L_e}{r}$)	Type of loading ***	Type **** of column
1	1a	260	182	0.7/2	2.95	91	compression	Long
	2b	260	182	0.78/2	3	91	combined	
2	2a	280	196	0.75/2	3.18	98	compression	
	2b	280	196	0.9/2	3.25	98	combined	
3	3a	300	210	0.76/2	3.38	105	compression	
	3b	300	210	0.85/2	3.43	105	combined	
4	4a	320	224	0.76/2	3.58	112	compression	
	4b	320	224	0.69/2	3.55	112	combined	
5	5a	340	238	1.48/2	4.14	119	compression	
	5b	340	238	0.94/2	3.87	119	combined	
6	6a	360	252	0.18/2	3.69	126	compression	
	6b	360	252	1.35/2	4.275	126	combined	
7	6a	380	266	1.43/2	4.52	133	compression	
	4b	380	266	1.5/2	4.55	133	combined	
8	5a	400	280	1.26/2	4.63	140	compression	
	5b	400	280	1.38/2	4.69	140	combined	
9	6a	420	294	1.45/2	4.93	147	compression	
	6b	420	294	1.4/2	4.9	147	combined	
10	7a	440	308	1.58/2	5.19	154	compression	
	7b	440	308	2.0/2	5.4	154	combined	
11	8a	460	322	0.6/2	4.9	161	compression	
	8b	460	322	2.1/2	5.65	161	combined	

* $L_e = KL$

** $\delta_{cr}(mm) = (L * 1\%) + \delta_o$

*** Compression load= axial compression load +torsion.

Combined load= (axial compression + bending load (at mid span)+torsion

**** $\lambda_c = \pi \sqrt{\frac{E}{\sigma_{pl}}} = 86.5$, if $\lambda_e > \lambda_c \rightarrow$ long column

Table 5,
Geometrical dimensions and buckling parameters of specimens type (2).

symbol	No.	T_{HD} (°C)	t_{HD} (min)	L (mm)	L_e (mm)	δ_o (mm)	δ_{cr}^* (mm)	λ_e	Type of column	Type of loading
A1	1	700	1	440	308	1.85/2	5.3	154	Long	Compression
	2	700	2			1.9/2	5.4			
	3	700	3			1.1/2	5			
	4	700	4			2.1/2	5.5			
	5	700	5			1.4/2	5.1			
B1	6	740	1	440	308	1.95/2	5.4	154	Long	Compression
	7	740	2			2.52/2	5.7			
	8	740	3			0.18/2	4.5			
	9	740	4			0.76/2	4.8			
	10	740	5			1.5/2	5.2			
C1	11	780	1	440	308	1.5/2	5.3	154	Long	Compression
	12	780	2			1.92/2	5.4			
	13	780	3			1.45/2	5			
	14	780	4			1.7/2	5.3			
	15	780	5			2.15/2	5.5			
D1	16	820	1	440	308	2.5/2	5.7	154	Long	Compression
	17	820	2			1/2	4.9			
	18	820	3			1/2	4.9			
	19	820	4			1.7/2	5.3			
	20	820	5			1.8/2	5.3			
E1	21	860	1	440	308	1.1/2	5	154	Long	Compression
	22	860	2			2.3/2	5.6			
	23	860	3			1.45/2	5			
	24	860	4			0.6/2	4.7			
	25	860	5			2.7/2	5.8			
A2	26	700	1	440	308	2.12/2	5.3	154	Long	Combined
	27	700	2			0.45/2	5.4			
	28	700	3			1.25/2	5			
	29	700	4			1.9/2	5.5			
	30	700	5			1.8/2	5.1			
B2	31	740	1	440	308	1.6/2	5.4	154	Long	Combined
	32	740	2			2.27/2	5.7			
	33	740	3			0.6/2	4.5			
	34	740	4			1.1/2	4.8			
	35	740	5			1.75/2	5.2			
C2	36	780	1	440	308	1.9/2	5.3	154	Long	Combined
	37	780	2			1.8/2	5.4			
	38	780	3			1.95/2	5			
	39	780	4			1.95/2	5.3			
	40	780	5			1.78/2	5.5			
D2	41	820	1	440	308	2.9/2	5.7	154	Long	Combined
	42	820	2			2.15/2	4.9			
	43	820	3			1.4/2	4.9			
	44	820	4			1.23/2	5.3			

	45	820	5			1.57/2	5.3			
E2	46	860	1	440	308	0.9/2	5	154	Long	Combined
	47	860	2			1.55/2	5.6			
	48	860	3			2.6/2	5			
	49	860	4			2.2/2	4.7			
	50	860	5			2.25/2	5.8			

$$* \delta_{cr}(mm) = (L * 1\%) + \delta_o$$

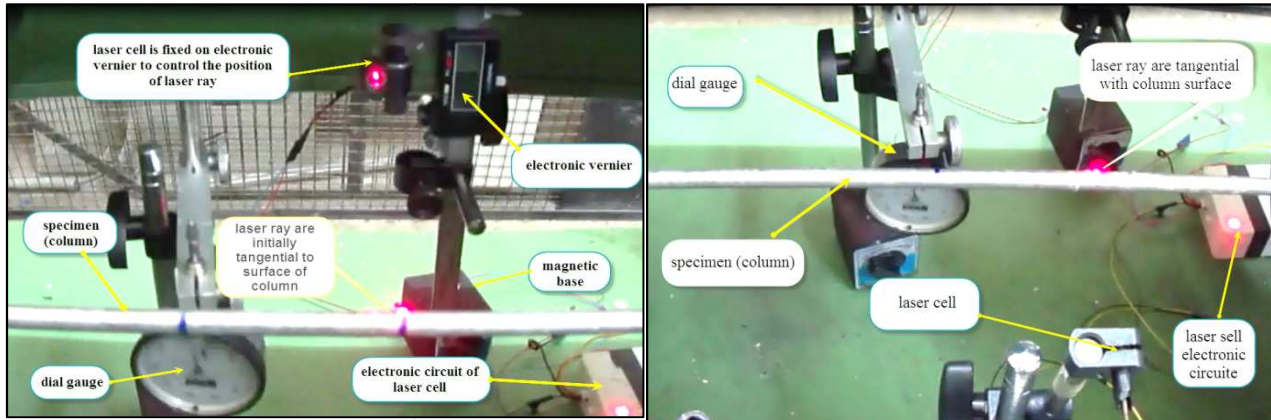


Fig. 4. System used to control the deflection of columns during buckling test.

4. Results and Discussion

Table (6) shows the experimental results of dynamic buckling test of 303 AISI column specimens without aluminizing (type 1). In Table (6) it can be observed that The critical buckling stress (σ_{cr}) decreased with increasing in effective slenderness ratio (λ_e) for both dynamic compression load (compression-torsion load) and dynamic combined load (compression-bending-torsion load). Also it can be seen that the bending load ($\sigma_{ben.}$) is greater than the critical buckling stress for all slenderness ratio, but is also decreased with increased in λ_e . In order to make a comparison between the experimental results and theoretical results, Eq. (1) is used to calculate the theoretical critical buckling stress for the specimens of type (1). The results of Eq. (1) and Eq. (2) are shown in Table (7). From Table (6) and Table (7), it can be observed that the experimental critical stress (σ_{exp}) is, in general, lower than the value of theoretical critical stress (σ_{cr}) from Perry Robertson interaction formula. The difference between the experimentally and theoretically results (Perry Robertson critical buckling stress) is duo to: initial imperfection of columns, the accuracy of construction of test machine, the alignment of loads, and the details of support condition which are not perfect as

assumed in theoretical consideration. Greenhill formula (Eq. 8) is used to fit the experimental results of the specimen's type (1) to find a mathematical model that describes the buckling behavior of these specimens. Table (8) shows the values of k function that used to determine the fitted model, Fig. (5). The fitted model was in the form of $k = 1/(-3.48777 + 3.40067/P_{exp}/P_{Cr}^0)$ and the values of the predicated buckling load (P) are given in Table (9). The fitted model gives a good correlation between the experimental values and theoretical values for slenderness ratio (91-154) with maximum error of 5.757 %. Table (10) shows the experimentally results of dynamic buckling test of specimens type (2) (hot-dip aluminized long columns) with constant slenderness ratio of $\lambda_e = 154$ and different hot-dip conditions (dipping temperature and dipping time). From Table (10), it can be detected that there is enhancement in buckling resistance of long aluminized columns under both dynamic compression load (compression and torsion) and combined load (compression, bending, and torsion), but the results are approximately the same. Whatever, it appear that the aluminizing conditions at dipping time of ($t_{HD}=3$ min) and dipping temperature of ($T_{HD}=820^\circ\text{C}$) gives a maximum enhancement of dynamic buckling resistance for the specimens of type (2). In order

to show the improvement of dynamic buckling resistance of aluminized columns (type 2) compared with non-aluminized columns (type 1), Fig.(6) is plotted by using the experimental results of Table (6) for specimens type (1), and Table (10) for specimens type (2), whereas Table (7) gives the theoretical results from Perry Robertson interaction formula. The improvement, based on the average value of critical buckling stress, is as follow: (64.8 %) for long columns type (2), compared with columns type (1), under dynamic compression loading, and (56.6 %) for long columns type (2), compared with columns type (1), under dynamic combined loading, and (38.3 %) for long columns type (2) compared with Perry Robertson critical buckling stress. These enhancement ratios of buckling resistance are calculated by compared the values of critical buckling stress illustrated in Fig. (7). It should be

noted that the effect of rotating of the column (torsional loading) during the applied of compression load and/or compression-bending loads was appear clearly first by a Spatial (non-planar) shape of column deformation until buckling is occur and second by reduced the value of the critical buckling load. The lateral loading (bending load) on rotating columns leads to a fast increasing in the lateral deflection of the column under combined loading conditions and a signification reduction in axial compressive load and as a result decrease the buckling resistance of the columns compared with the case without lateral loading . It experimentally noted that the effect of the lateral loading on the buckling resistance was much greater than the effect of the twisting or torsional loading for the same slenderness ratios.

Table 6,
Experimental results of dynamic buckling test of column specimen type (1).

No.	Symbol	P_{exp} (N)	σ_{exp} (Mpa)	$F_{ben.}$ (N)	$\sigma_{ben.}$ (Mpa)
1	1a	7422.0126	147.6563	---	---
	1b	4523.893	90	306	247.312
2	2a	6785.8401	135	---	---
	2b	4241.15	84.375	285.6	248.58
3	3a	6008.296	119.5313	---	---
	3b	3887.721	77.3438	265.2	247.312
4	4a	5301.4376	105.4688	---	---
	4b	3534.292	70.3125	244.8	243.507
5	5a	4948.0084	98.4375	---	---
	5b	3322.234	66.0938	224.4	237.166
6	6a	4665.2651	92.8125	---	---
	6b	3180.863	63.2813	204	228.288
7	7a	4241.1501	84.375	---	---
	7b	3039.491	60.4688	183.6	216.874
8	8a	3887.7209	77.34375	---	---
	8b	2827.433	56.25	163.2	202.923
9	9a	3534.2917	70.3125	---	---
	9b	2686.062	53.4375	142.8	186.435
10	10a	3180.8626	63.28125	---	---
	10b	2474.004	49.2188	122.4	167.411
11	11a	2827.4334	56.25	---	---
	11b	2120.575	42.1875	81.6	116.68

Table 7,
Theoretical values of critical load and critical stress using Perry Robertson interaction formula for specimen type (1).

No.	L (mm)	L _e (mm)	$\lambda_e(\frac{L_e}{r})$	P _{cr} (N)	σ_{cr} (Mpa)
1	260	182	91	9764.33	194.2552
2	280	196	98	8602.489	171.1411
3	300	210	105	7625.835	151.7112
4	320	224	112	6800.153	135.2848
5	340	238	119	6097.662	121.3091
6	360	252	126	5496.088	109.3412
7	380	266	133	4977.642	99.02704
8	400	280	140	4528.094	90.08358
9	420	294	147	4136.02	82.28352
10	440	308	154	3792.199	75.44341
11	460	322	161	3489.142356	69.41429

Table 8,
Theoretical values of Greenhill formula for specimen type (1).

No.	L (mm)	L _e (mm)	$\lambda_e(\frac{L_e}{r})$	P _{exp} (N)	P _{cr} ⁰ (N)	P _{exp} /P _{cr} ⁰	M _t [*] (N.mm)	k
1	260	182	91	7422.012644	12233.2698	0.606707182	209523	0.471332517
2	280	196	98	6785.840132	10548.07447	0.643325012	209523	0.533008048
3	300	210	105	6008.29595	9188.544868	0.65388982	209523	0.579730475
4	320	224	112	5301.437603	8075.869513	0.656454094	209523	0.620682717
5	340	238	119	4948.00843	7153.711403	0.691670121	209523	0.696118496
6	360	252	126	4665.265091	6380.933936	0.731125747	209523	0.789296097
7	380	266	133	4241.150083	5726.932397	0.740562275	209523	0.848162555
8	400	280	140	3887.720909	5168.556489	0.752186983	209523	0.913503038
9	420	294	147	3534.291735	4688.033096	0.753896498	209523	0.962503809
10	440	308	154	3180.862562	4271.534288	0.744665113	209523	0.989941795
11	460	322	161	2827.433388	3908.171258	0.723467116	209523	0.994481029

* For motor power of 0.5 KW and N=17 r.p.m

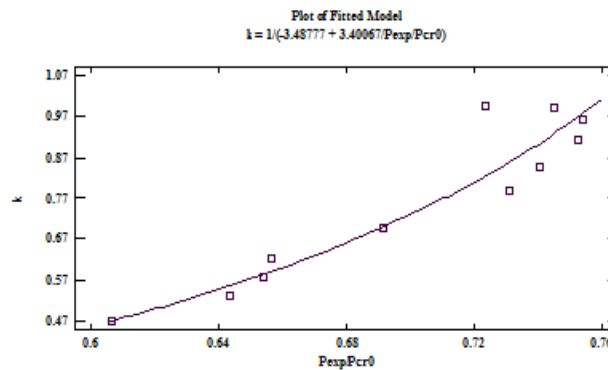


Fig. 5. Function k predicated using Greenhill formula results.

Table 9,
Theoretical results of fitted model ($k = 1/(-3.48777 + 3.40067/P_{exp}/P_{cr}^0)$).

No.	L (mm)	L_e (mm)	k	M_{cr}^0 (N.mm)	P (fitted model) (N)	P_{exp} (N)	Error%
1	260	182	0.472287209	334774.5823	7441.032476	7422.012644	0.296
2	280	196	0.556076439	366012.6571	7091.215227	6785.840132	4.500
3	300	210	0.583802725	358644.7718	6052.238726	6008.29595	0.731
4	320	224	0.590809751	340265.0296	5013.515634	5301.437603	-5.431
5	340	238	0.699870006	379365.7378	4971.40402	4948.00843	0.472
6	360	252	0.859468903	439994.5612	4933.861242	4665.265091	5.757
7	380	266	0.905599535	439210.0157	4423.530637	4241.150083	4.300
8	400	280	0.967798059	445907.1091	4027.305436	3887.720909	3.590
9	420	294	0.977496457	428929.1311	3569.315935	3534.291735	0.990
10	440	308	0.926835156	388212.4536	3027.175305	3180.862562	-4.831
11	460	322	0.824573802	330362.9546	2336.029801	2827.433388	-17.3798

Table 10,
Experimental results of dynamic buckling test of column specimen type (2).

symbol	No.	P_{exp} (N)	σ_{exp} (Mpa)	symbol	No.	P_{exp} (N)	σ_{exp} (Mpa)	F_b (N)	σ_{be} (Mpa)
A1	1	5655	112.5	A2	26	3534.292	70.3125	163.2	357.1437
	2	6362	126.5625		27	3534.292	70.3125	204	446.4297
	3	5655	112.5		28	3534.292	70.3125	183.6	401.7867
	4	4948	98.4375		29	4241.15	84.375	163.2	357.1437
	5	4948	98.4375		30	4241.15	84.375	204	446.4297
B1	6	4948	98.4375	B2	31	3534.292	70.3125	204	446.4297
	7	4241	84.375		32	3534.292	70.3125	183.6	401.7867
	8	4948	98.4375		33	4241.15	84.375	183.6	401.7867
	9	5655	112.5		34	4241.15	84.375	204	446.4297
	10	5655	112.5		35	3534.292	70.3125	163.2	357.1437
C1	11	4948	98.4375	C2	36	4241.15	84.375	204	446.4297
	12	5301	105.4688		37	3534.292	70.3125	183.6	401.7867
	13	5655	112.5		38	4241.15	84.375	183.6	401.7867
	14	5301	105.4688		39	2827.433	56.25	163.2	357.1437
	15	4948	98.4375		40	2827.433	56.25	204	446.4297
D1	16	5655	112.5	D2	41	4241.15	84.375	183.6	401.7867
	17	7069	140.625		42	4241.15	84.375	204	446.4297
	18	4948	98.4375		43	4948.008	98.4375	183.6	401.7867
	19	4948	98.4375		44	4241.15	84.375	204	446.4297
	20	5301	105.4688		45	4241.15	84.375	204	446.4297
E1	21	5655	112.5	E2	46	4241.15	84.375	204	446.4297

22	4948	98.4375	47	4241.15	84.375	183.6	401.7867
23	4948	98.4375	48	4241.15	84.375	204	446.4297
24	4241	84.375	49	3534.292	70.3125	163.2	357.1437
25	4241	84.375	50	2827.433	56.25	204	446.4297

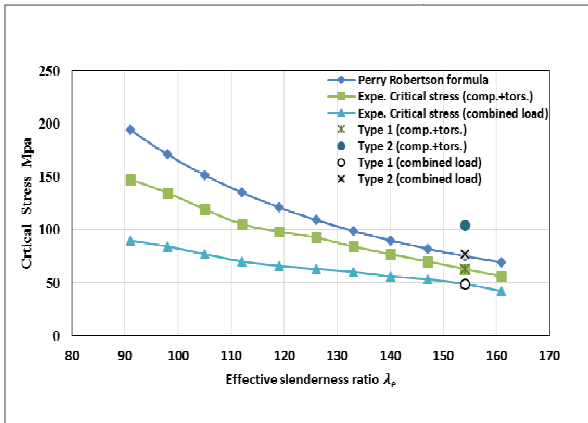


Fig. 6. Critical stress- slenderness ratio relation for stainless steel 303 AISI columns under dynamic compression and combined loads compared with theoretical results (Perry Robertson formula).

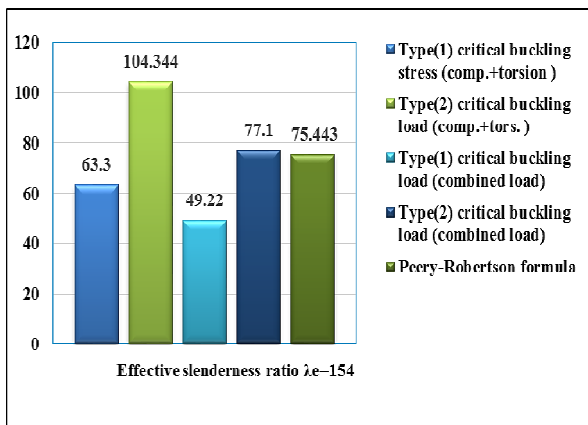


Fig. 7. Critical buckling stress for the specimens of type (1) and type (2) at the same effective slenderness ratio.

5. Conclusions

1. The experimental values of the critical buckling loads and/or stresses for non-aluminized long columns, ($\lambda_e > \lambda_c, \lambda_e(91 \text{ to } 161)$), are less than the theoretical values predicated by Perry Robertson interaction formula, and this differences in results is duo to effect of initial imperfection of columns, the accuracy of

- construction of test machine, the alignment of loads, and the details of support condition.
- Using of hot- dip aluminizing surface treatment has make double benefit one of them is to develop protection layer for substrate material from environment conditions and the other is the improvement of dynamic buckling resistance of long aluminized columns under dynamic compression loading and under dynamic combined loading.
 - The improvement in the dynamic buckling resistance were (64.8 %) for long columns type (2), compared with columns type (1), under dynamic compression loading only, and (56.6 %) for long columns type (2), compared with columns type (1), under dynamic combined loading, and (33.3 %) for long columns type (2) compared with Perry Robertson critical buckling stress.
 - The optimum hot-dip aluminizing conditions, that give a maximum enhancement of dynamic buckling resistance for the specimens of type (2), are: dipping time of ($t_{HD}=3 \text{ min}$) and dipping temperature of ($T_{HD}=820^\circ\text{C}$).
 - torsional loading during the applied of compression load and/or compression-bending loads was appear clearly first by a Spatial (non-planar) shape of column deformation until buckling is occur and second by reduced the value of the critical buckling load.
 - The lateral loading (bending load) on rotating columns leads to a fast increasing in the lateral deflection of the column under combined loading conditions and a signification reduction in axial compressive load (critical buckling load).

Notation		
T_{HD}	Dipping temperature	°C
t_{HD}	Dipping time	s (second)
P_{cr}, P_{exp}	Theoretical and experimental critical buckling load	N (newton)
A	The cross-sectional area of the column	mm²
E	Modulus of elasticity	GPa
K	Effective length factor (depends on column ends support)	dimensionless
L, L_e	Unsupported and effective length of the column	mm
r	Smallest radius of gyration of the column	mm
I	Moment of inertia of the column cross sectional area	mm⁴
P_{cr}^0	critical load for buckling without torque (Euler formula)	N
M_t	Applied torque	N.mm
M_{cr}^0	critical torque for buckling without axial force	N.mm
F_b	Bending load	N

Greek letters

$\sigma_{cr}, \sigma_{exp}$	Theoretical and experimental critical buckling stress	MPa
χ	The reduction factor accounting for buckling	dimensionless
σ_y	the yield strength	MPa
α	The imperfection factor defined in table (3-1).	dimensionless
$\bar{\lambda}_o, \bar{\lambda}$	The limiting and non-dimensional slenderness ratio	dimensionless

λ_e, λ_c	Effective and critical slenderness ratio	dimensionless
$\sigma_{ult}, \sigma_{pl}$	Ultimate and proportional limit of column's material	MPa
δ_o, δ_{cr}	Initial and critical deflection of the column	mm
σ_b	Bending stress = F_b/A	MPa

6. References

- [1] T. H. G. MEGSON, "Structural and Stress Analysis", Butterworth-Heinemann, 2000.
- [2] Jianqiao Ye, "Structural and Stress Analysis Theories, tutorials and examples", Taylor & Francis, 2008.
- [3] R. C. Hibbeler, SI conversion by S. C. Fan, "Statics and Mechanics of Materials", Prentice-Hall, Inc., 2004.
- [4] N. R. Baddoo, "A Comparison of Structural Stainless Steel Design Standards", the Steel Construction Institute, p.p. 131-149, (2003).
- [5] L. Gardner and D. A. Nethercot, "Experiments on Stainless Steel Hollow Sections-Part 2: Member Behaviour of Columns and Beams", Journal of Constructional Steel Research, Vol. 60, p.p. 1319-1332, (2004).
- [6] Kifah Hameed Al-Jubori, "Columns Lateral Buckling Under Combined Dynamic Loading", PhD. Thesis, University of Technology, Department of Technical Education, 2005.
- [7] Hamed Ali Hussein, "Buckling of Square Columns Under Cycling Loads for Nitriding Steel DIN (CK45, CK67, CK101)", PhD. Thesis, University of Technology, Department of Mechanical Engineering, 2010.
- [8] Al-Alkhawi H. J. M., Al-Khazraji A. N., and Essam Zuhier Fadhel, "Determination the Optimum Shot Peening Time for Improving the Buckling Behavior of Medium Carbon Steel", Eng. & Tech. Journal, Vol. 32, Part (A), No. 3, 2014.
- [9] Sung-Ha Hwang, Jin-Hwa Song, and Yong-Suk Kim, "Effects of carbon content of carbon steel on its dissolution into a molten aluminum alloy", Materials Science and Engineering A 390, pp. 437-443, 2005.

- [10] Hishamuddin Hj. Husain, Muhamad Daud, Anasyida Abu Seman and Abdul Razak Daud, "Preliminary Study on Metallic Coating of Steel Substrates through Hot Dip Aluminizing by Using Energy Dispersive X-Ray Spectroscopy (EDX) Technique", *Journal of Nuclear and Related Technologies*, Vol. 6, No. 2, pp. 63-69, December, 2009.
- [11] Rajab Mohammed Hussein, "Improvement of Stainless Steel (316L) Hot Corrosion and Oxidation Resistance by Aluminizing-Siliconizing", PhD. Thesis, University of Technology, Department of Production Engineering and Metallurgy, 2007.
- [12] G. H. Awan, F. Ahmed, L. Ali, M. S. Shuja, and F. Hasan, "Effect of Coating-Thickness on the Formability of Hot Dip Aluminized Steel", *Pak. J. Engg. & Appl. Sci.*, Vol. 2, p.p. 14-21, Jan 2008.
- [13] N. R. Baddoo and B. A. Burgan, "Structural Design of Stainless Steel", The Steel Construction Institute, SCI Publication P291 2001, 2001.
- [14] Euro Inox and The Steel Construction Institute, "Structural Design of Stainless Steel", 3rd edition, 2006.
- [15] L. Gardner and D. A. Nethercot, "Designers' Guide to EN 1993-1-1. Eurocode 3: Design of Steel Structures. General Rules and Rules for Building", The Steel Construction Institute, Thomas Telford Ltd., 2005.
- [16] James M. Gere, "Mechanics of Materials", 6th Ed, Thomson Learning, Inc., 2004.
- [17] Zdeněk P. Bažant and Luigi Cipolin "Stability of Structures Elastic, Inelastic, Fracture, and Damage theories", Dover Publications, Inc., 2003.
- [18] ASM Handbook, "Surface Engineering", ASM International, Vol. 5, 1994.

تحسين مقاومة الانبعاج للاعمدة الطويلة من الصلب المقاوم للصدأ AISI 303 المؤلمة بطريقة الغمر الساخن (HDA)

احمد نايف الخزرجي* سمير علي الربيعي** حميد شمخي جابر الخزعلي***

، قسم الهندسة الميكانيكية / الجامعة التكنولوجية / بغداد
 *** قسم المكنات والمعدات / معهد التكنولوجيا / الجامعة التقنية الوسطى / بغداد
 *البريد الالكتروني: dr_ahmed53@yahoo.com
 **البريد الالكتروني: alrabiee202@yahoo.com
 ***البريد الالكتروني: hameedshamkhi@yahoo.com

الخلاصة

تم في هذا البحث التحقق العملي لسلوك الانبعاج الديناميكي للاعمدة الطويلة المؤلمة وغير المؤلمة المصنوعة من الصلب المقاوم للصدأ AISI 303 . حيث فحصت هذه الاعمدة تحت تأثير حمل الانبعاج الديناميكي، ٢٢ عينة غير مؤلمة (type 1) و ٥٠ عينة مؤلمة بطريقة الغمر الساخن (type 2)، وبظروف غمر مختلفة من درجة حرارة الغمر وزمن الغمر، باستخدام ماكينة فحص الانبعاج الدوار ولحالة حمل الانضغاط الديناميكي وكذلك الحمل المركب (حمل انضغاط زائد حمل انحناء). تم مقارنة النتائج مع صيغة Perry Robertson interaction formula. تم استخدام صيغة Greenhill لغرض الحصول على موديل رياضي يصف سلوك الانبعاج تحت تأثير حمل الانبعاج الديناميكي. أظهرت النتائج الفائدة العملية المتحققة من عملية الالمنة بالغمر الساخن على سلوك الانبعاج تحت تأثير الاحمال الديناميكية. تمثل هذا التأثير الايجابي بتحسين مقاومة الانبعاج الديناميكي للاعمدة الطويلة المستخدمة في هذا البحث بنسب مئوية لمتوسط اجهاد الانبعاج الحرج، وهذه النسب كما يلي: (64.8 %) للاعمدة الطويلة نوع (٢) مقارنة بالاعمدة نوع (١) وتحت تأثير التحميل الانضغاطي الديناميكي، و (56.6 %) للاعمدة الطويلة نوع (٢) مقارنة بالاعمدة نوع (١) وتحت تأثير التحميل الديناميكي المركب، و (33.3%) للاعمدة نوع (٢) مقارنة بقيمة اجهاد الانبعاج الحرج المحسوب من صيغة Perry Robertson.